STRESSES IN A QUARTER-INFINITE PLATE FOR A LOADED HOLE

by

William Eugene Brunschwyler III

A Thesis Submitted for Partial

Fulfillment for the Degree of

MASTER OF SCIENCE

in

APPLIED MECHANICS

Approved:

_____

In Charge of Investigation

_____

Head of Major Department

_____

Dean of Engineering Division

_____

Director of Graduate Studies

Virginia Polytechnic Institute

Blacksburg, Virginia

1949

146309

TABLE OF CONTENTS

FIGURES

TABLES

Explanation of Symbols

a— width of margin.

d— diameter of hole.

P— applied load.

A— area of hole.

ϕ— load angle.

F— model fringe constant (p.s.i., shear).

t— thickness of plate.

y— denotes vertical direction, parallel to direction of applied load.

x—denotes direction perpendicular to y-direction.

τ_{xy}— shear stress on a plane parallel to y-direction.

σ_x, σ_y—normal stresses in x and y-directions, respectively.

θ— isoclinic parameter.

θ_y— angle between y-direction and principal stress direction.

(P-Q)—principal stress difference.

β—angle between stress trajectory and isoclinic line.

b—fringe value

Isochromatic pattern.
($\phi=270^{o}$)

I. INTRODUCTION

This thesis presents the results of an investigation of marginal stresses in a flat plate. The stresses consist of tension, compression and shear. Values of the stresses are primarily functions of the applied loads and margin widths. Minor factors affecting them are clearance between the loading plate and hole surface, ratio of plate thickness to hole diameter and the amount of friction between surfaces of the pin and hole. The minor factors were not varied for this work and the results are presented in terms of P/A and a/d. 'P' is the applied load, 'A' is the area of the hole, 'a' is the width of the margin and 'd' is the diameter of the hole.

Since the model was made of bakelite, there will be some error in transposing the results to a prototype of a different material. The error is due to the fact that the materials do not have the same values for Poisson's ratio and modulus of elasticity.* However, Frocht[11] proved that the error is negligible for all practical purposes.

Photoelastic methods were used to evaluate the stresses.

*The modulus of elasticity affects the results only when the plate and pin are made of different materials.

II. REVIEW OF LITERATURE

Although problems similar and related to the one presented herein could be found in publications, no data which showed marginal stresses in a flat plate as a function of $^{a}/_{d}$ could be located.

Frocht[1] analyzed the stresses around a hole in the head of a flat bar which was loaded in a manner similar to the method used in this investigation. However, in his problem the stresses were dependent on the dimension of the bar perpendicular to the line of the load rather than the width of the margin in the direction of the load.

Bickley[2] and Knight[3] investigated the stresses around internally loaded holes in flat plates, but neither gave the effect of the margin width. Coker[4] also made a study of stresses near holes in flat plates but confined his results to phases of the stress distribution other than its variation with width of margin.

Seely[5] suggested a means of design by saying "experience has shown that if the width of margin is $1^{1}/_{2}$ to 2 times the diameter of the rivet, the joint will not fail in the margin." Bruhn[6], Younger[7] and Marks[8] also gave the minimum $^{a}/_{d}$ ratio as $1^{1}/2$ but none presented any data to substantiate his statements or gave any indication as to the stress distribution in a margin.

Coker[4] showed results of an investigation of stresses with varying plate thickness to hole diameter ratio. They showed that the ratio must be relatively high to prevent buckling of the plate.

By reference to Frocht[9] it can be noted that the stresses around a hole in a plate loaded by a pin with 0.002" clearance (same as used in this experiment) will be about 15% higher than those with no clearance. He also

showed, in the same reference[9], that the stresses continued to increase with clearance, although not as rapidly, and that a very slight decrease is caused in the stresses by lubricating the hole to decrease friction.

III. RESULTS

Curves in Figures 1, 2 and 3 show the results of the investigation.

Curves in Fig. 1 show the variation of the maximum shear stress that occurs in the plate model for various $^{a}/_{d}$ ratios. The stress concentration factor (ordinate) is the ratio of the maximum shear stress in the plate to $^{P}/_{A}$. The maximum shear stress was determined by multiplying the maximum fringe order by the fringe constant in pounds per square inch, shear.

Curves in Fig. 2 give the variation of the maximum tensile stress in the plate with the $^{a}/_{d}$ ratio. Again the SCF is based on $^{P}/_{A}$. The value of maximum tensile stress was obtained by use of Mesnager's theorem.* (See discussion of results).

Curves in Fig. 3 give the variation of the maximum compressive stress in the model with $^{a}/_{d}$. The SCF is based on $^{P}/_{A}$. The point of maximum compressive stress was obtained by use of Mesnager's theorem* and its value was found by graphical integration using Lamé-Maxwell(10) equations.

No curves are shown for load angles of ϕ = 0 degrees, 270 degrees and 315 degrees since the marginal stresses are not critical for those conditions.

---

*See "Photoelasticity", Vol. I, by M. M. Frocht, p. 215, John Wiley & Sons, Inc., N. Y., 1941.

SHEAR STRESS CONCENTRATION FACTOR

versus

a/d RATIO

S.C.F.(S)= maximum shear stress divided by P/A

(P=applied load)

(A=area of hole)

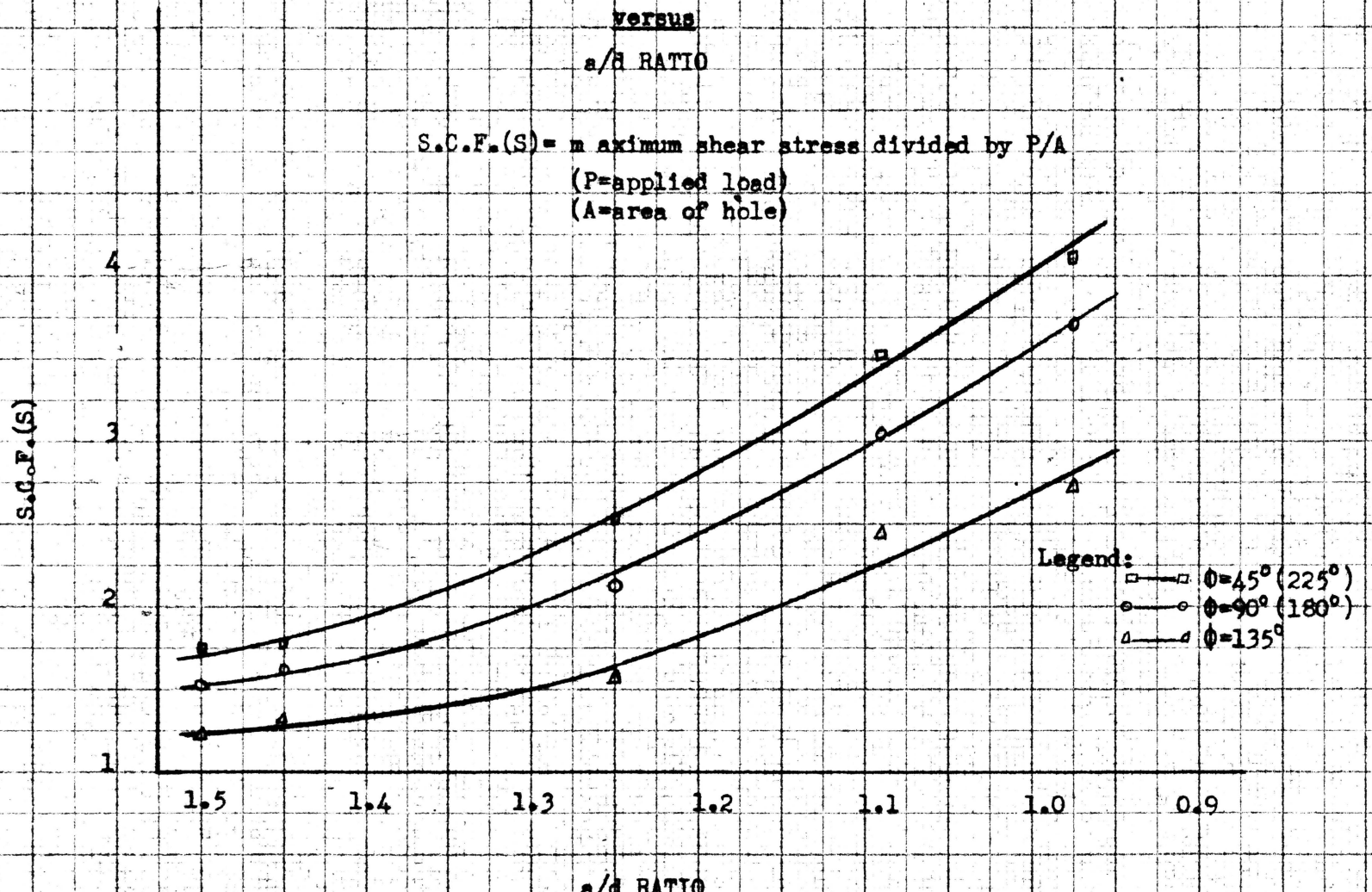

Fig. 4

KEUFFEL & ESSER CO. N.Y.

TENSILE STRESS CONCENTRATION FACTOR

versus

a/d RATIO

S.C.F.(T)=maximum tensile stress/P/A

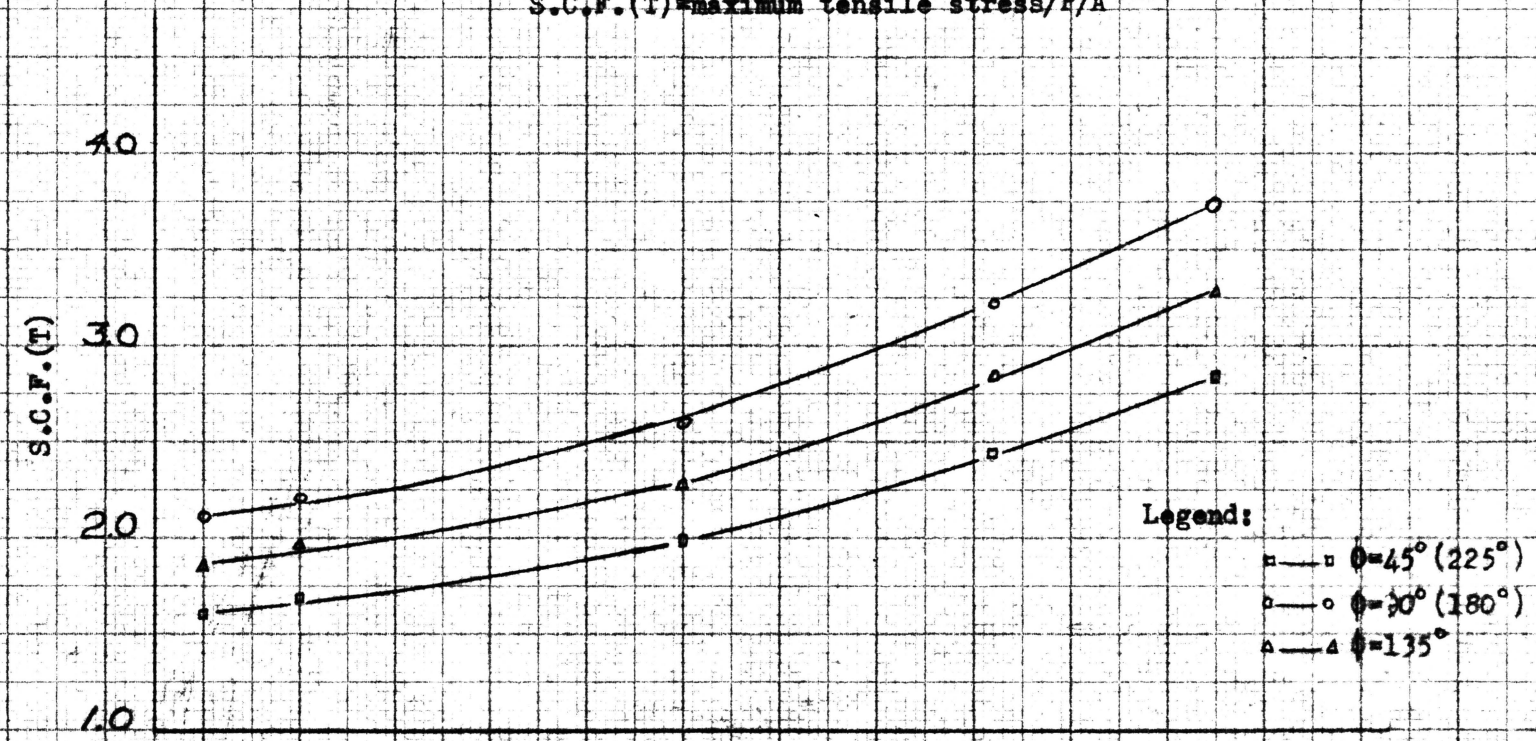

Fig. 2.

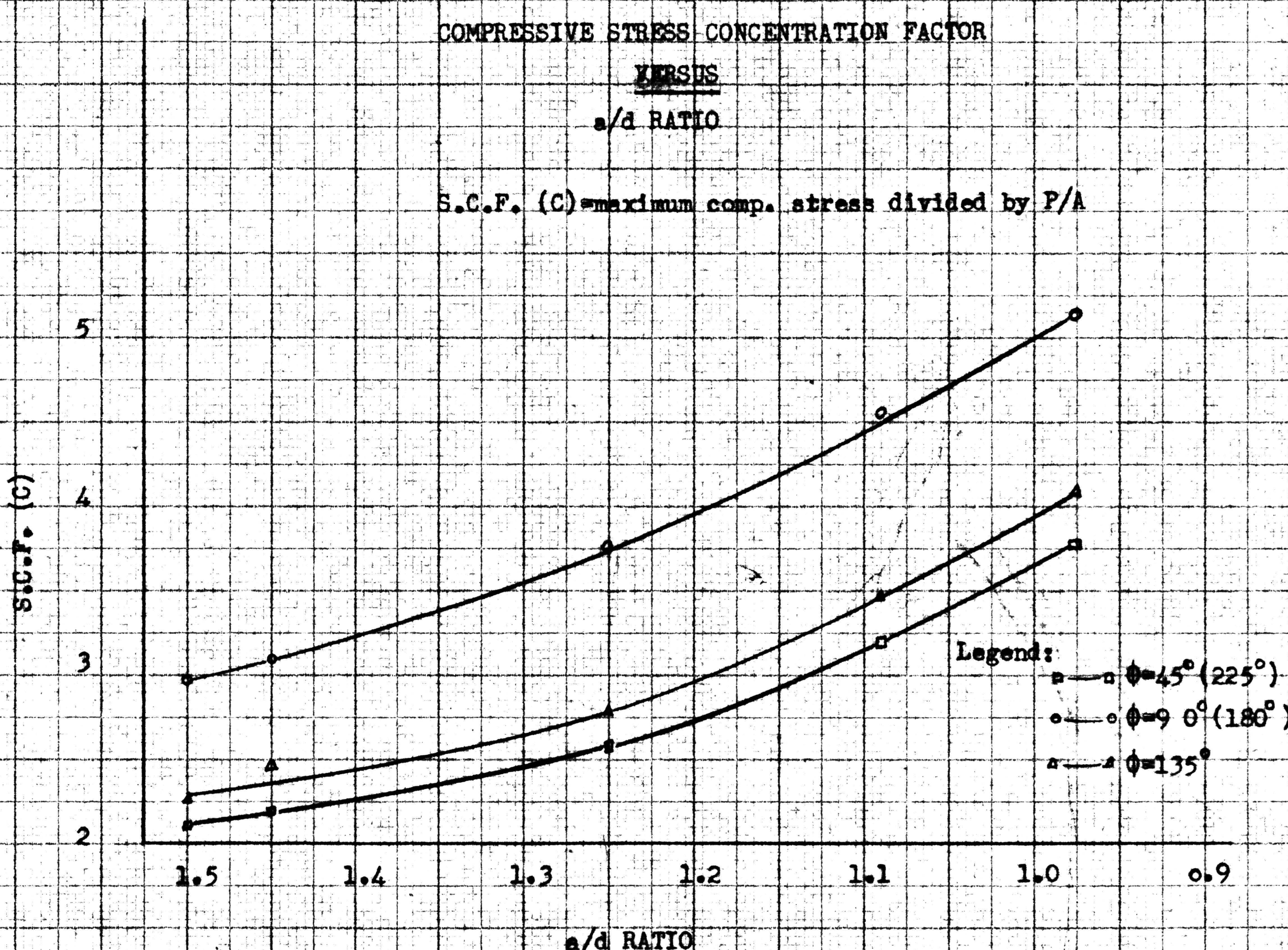
COMPRESSIVE STRESS CONCENTRATION FACTOR
VERSUS
a/d RATIO
S.C.F. (C)=maximum comp. stress divided by P/A
S.C.F. (C)
5
4
3
2
1.5
1.4
1.3
1.2
1.1
1.0
0.9
a/d RATIO
Legend:
φ=45°(225°)
φ=90°(180°)
φ=135°

Fig. 3.

Table I

Tabulated values stress of concentration factors for different values of load angle ϕ and a/d.

	a/d=1.50 P=261# d=0.500" P/A=1310 F=165			a/d=1.453 P=261# d=0.514" P/A=1250 F=172			a/d=1.25 P=261# d=0.562" P/A=1060 F=172.5			a/d=1.09 P=261# d=0.625" P/A=850 F=172.5			a/d=0.975 P=261# d=0.672" P/A=738 F=172.5		
ϕ	SCF (S)	SCF (T)	SCF (C)	SCF (S)	SCF (T)	SCF (C)	SCF (S)	SCF (T)	SCF (C)	SCF (S)	SCF (T)	SCF (C)	SCF (S)	SCF (T)	SCF (C)
45° 225°	1.35	1.60	2.10	1.38	1.68	2.19	1.78	1.97	2.58	2.23	2.44	3.20	2.56	2.83	3.72
90° 180°	1.26	2.10	2.96	1.32	2.21	3.10	1.62	2.60	3.76	2.03	3.23	4.54	2.34	3.74	5.25
135°	1.15	1.85	2.26	1.18	1.94	2.49	1.29	2.28	2.79	1.62	2.84	3.47	1.87	3.28	4.10

IV. EXPERIMENTAL INVESTIGATION

A. Object of Investigation

The object of this investigation is to determine the magnitude of the shear, compressive and tensile stresses around a hole near the boundary in a flat plate as a function of $^{a}/_{d}$.

B. Procedure

1. Construction of model:

The model was cut from a sheet of bakelite (BT - 61-893) and supported in a metal frame as shown in Fig. 4. The method of support was chosen to approximate actual conditions under which a quarter infinite plate is approached. Hand reaming was used to obtain the final desired dimensions of the hole, and the sides were shaped by side milling using inward cutting. All drilling was performed under water to eliminate stresses due to heating.

Various $^{a}/_{d}$ ratios were obtained by increasing the diameter of the hole.

A plate with a thickness equal to 0.286" was used for $^{a}/_{d} = 1.5$. For all other ratios, t = 0.272".

2. Construction of loading device:

To obtain a clear picture of the stress pattern near the boundary of the hole, a bakelite bearing was made as shown in Fig. 5 and cut to give a clearance of 0.002". The pin to transmit the load to the bearing was made on a lathe from SAE 1090 steel. Since it was desired to get the stress pattern for the full 360 degrees of the hole, two means for loading the pin were devised so that one showed the area obscured by the other. (Refer to Fig. 5).

Holes were drilled in the metal frame supporting the model so that it could be placed in the loading machine at any desired angle. (The method of support for ϕ = 45 degrees (225 degrees) is shown in Fig. 6).

3. Loading:

Loads were applied on the specimen by means of a lever system, shown schematically in Fig. 6. The direction of the applied load is denoted by the angle ϕ, measured counterclockwise as shown in Fig. 7. It can be noted that the load for ϕ = 45 degrees gives the same result as for ϕ = 225 degrees, and that the same thing is true for ϕ = 90 degrees and ϕ = 180 degrees.

4. Isochromatics:

For each angle of the applied load the isochromatics were obtained by using the mercury arc lamp with a 5461 Å filter. A permanent record was made for the pattern by taking a picture for each load angle. Ortho X film, size 5" X 7", was used in a box camera with an exposure time of 25 seconds. The plates were developed immediately after exposure.

5. Isoclinics:

White light with no filter was used to obtain the isoclinics. The picture was focused on a sheet of vellum placed on a large glass plate, and the lines of constant principal stress directions were sketched on the vellum for parameters of 0 degrees to 90 degrees in increments of 10 degrees. The parameters were measured counterclockwise from the vertical. The isoclinic pattern was then drawn to scale on a smaller sheet.

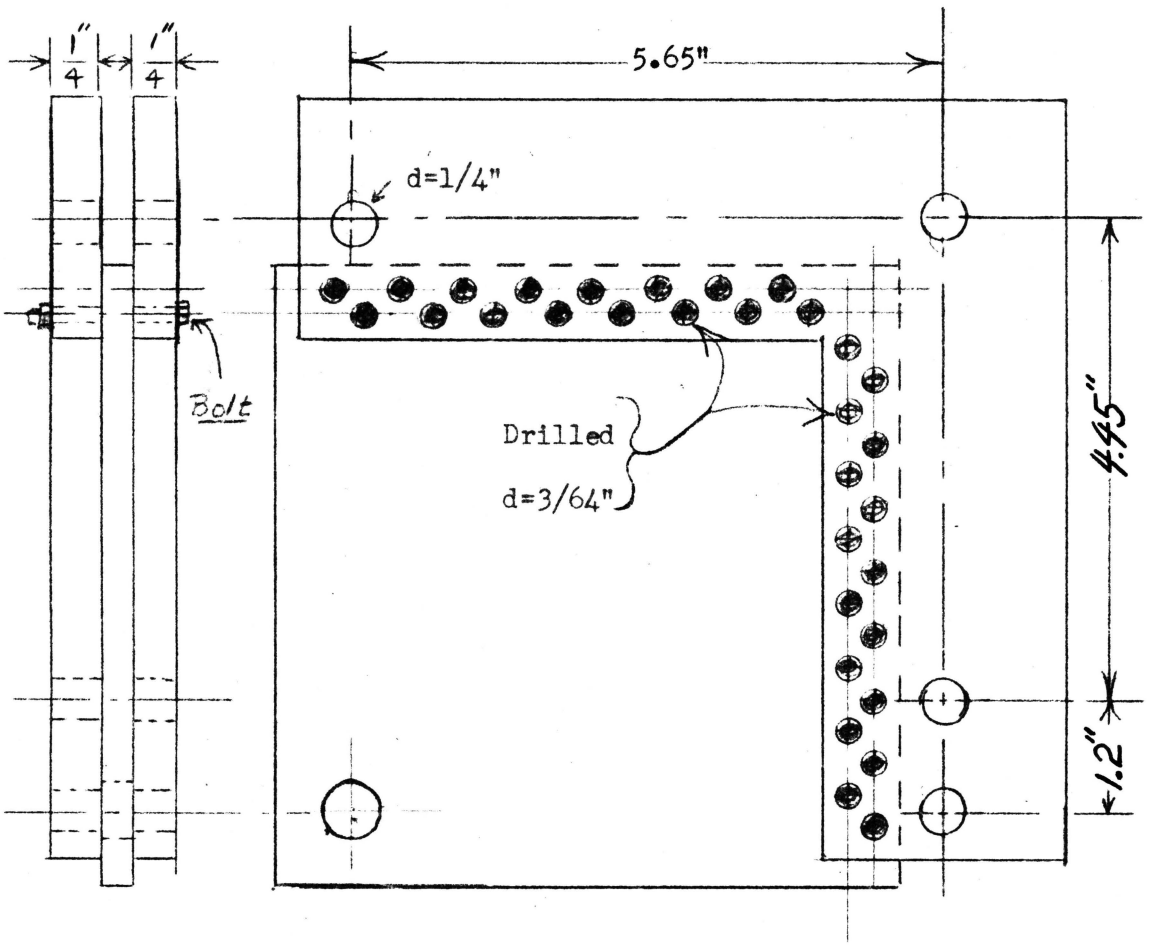

Fig. 4.

Sketch showing how bakelite plate was supported between two metal angles.

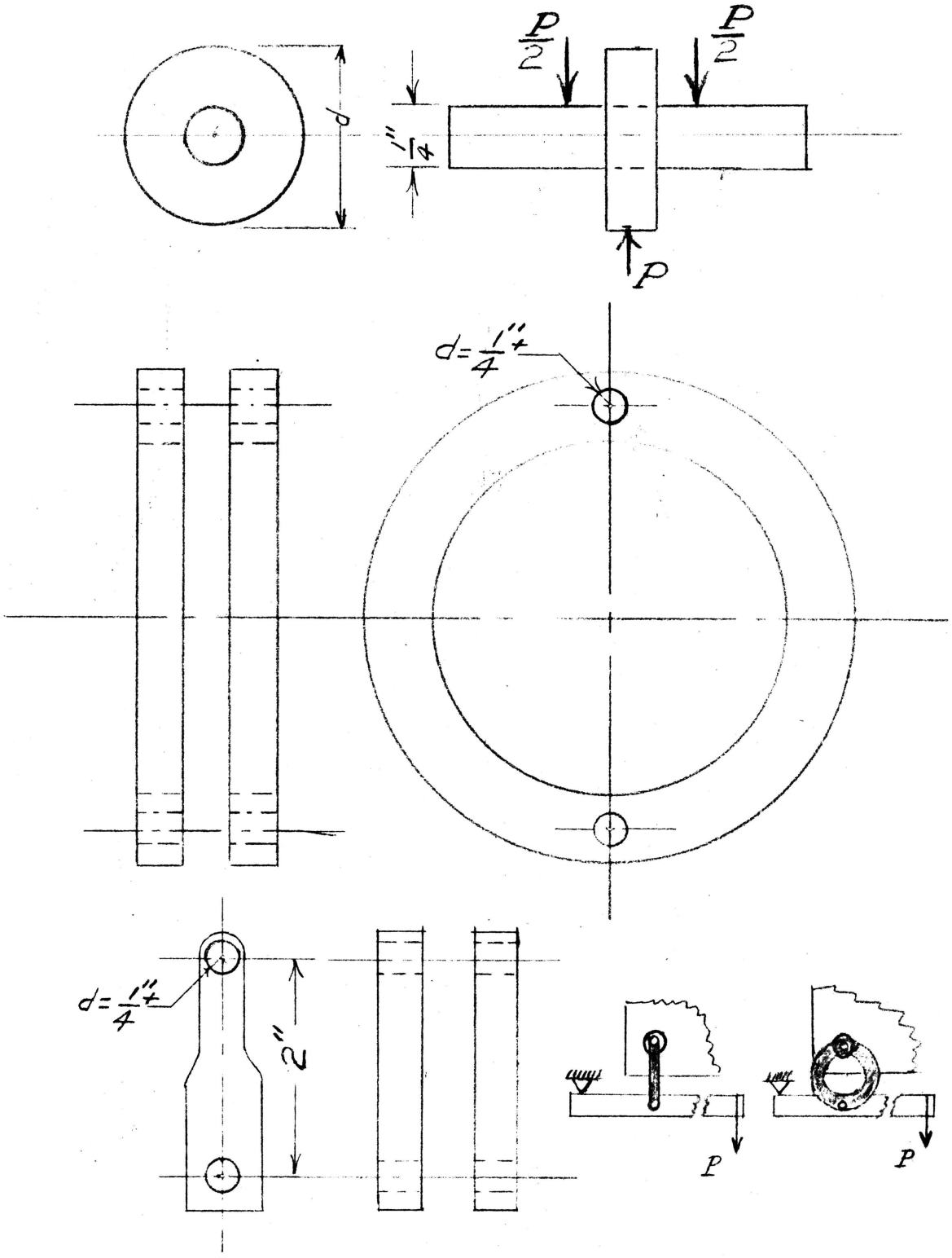

Fig. 5.

Sketch of bakelite bearing with loading pin, loading devices.

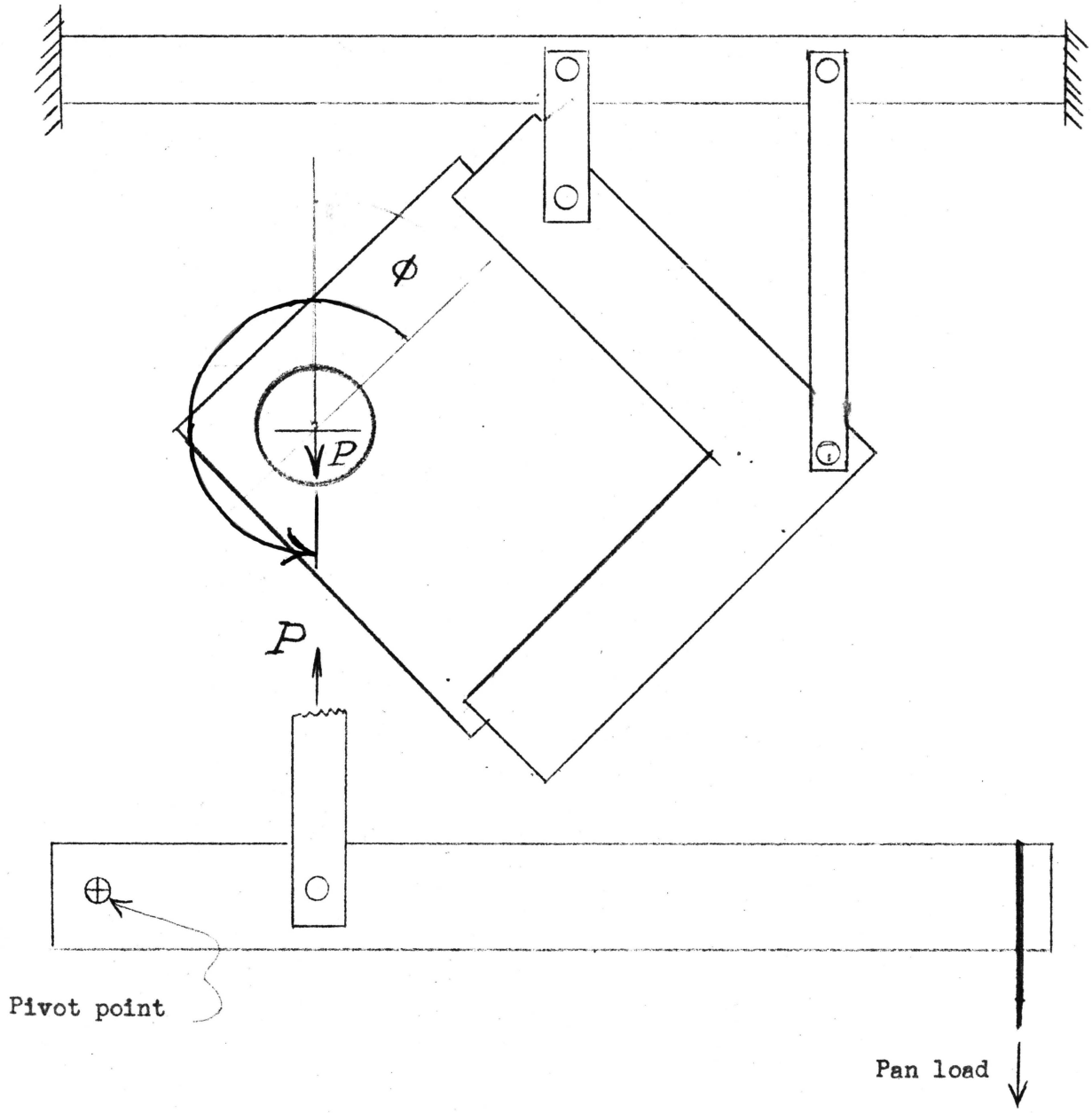

Fig. 6.

Sketch showing method of loading for ϕ=45(225) degrees.

C. Check On Results

To justify the results obtained, several checks were made to substantiate the accuracy of the photoelastic methods used.

1. Check on load 'P' by vertical shear:

For a check, the value of the applied load was compared to the summation of the vertical shear on the sections A'C' and AC (See Fig. 7) as determined from the isochromatic and isoclinic patterns for the load angle of ϕ = 180 degrees. The distances A'C' and AC were divided into thirteen stations and the values of the fringe order and the angle θ_y were determined for each station. From this, the value of shear stress was computed. Table 2 gives the data in tabular form and curves in Fig. 10 show the desired integrals of τ_{xy} versus Y for the two sections. It is obvious that the sum of the shear on these two faces should equal the value of 'P'. The areas under the two curves add up to 33.42 square inches. This area multiplied by the scale factor $\left(\frac{400}{6}\right)^2$ and the shear area (t = 0.286, Y = 1") gives the vertical shear equal to 638 pounds. The applied load was 623 pounds. The error is 2.1%.

2. Check on calculations of principal stresses by shear difference and graphical integration methods:

The principal stresses were determined at point 'B' (Fig. 7) by the shear difference and graphical integration methods. In this check, ϕ = 180 degrees.

In the shear difference method, use is made of the equilibrium equation:

$$d\sigma_y = \left[\partial(\tau_{xy})/\partial x\right] \cdot dy$$

The $\partial(\tau_{xy})/\partial x$ was determined for each station along the line OB. To obtain greater accuracy, the variation of τ_{xy} with 'x' was determined by

finding the values of τ_{xy} for two values of 'x' with Y = constant and assuming a parabolic variation of τ_{xy}. The slope of the parabola at X = 0 gives the desired $\partial(\tau_{xy})/\partial x$. This calculation is shown in tabular form in Table 3. The curve $\partial(\tau_{xy})/\partial x$ against ΔY, as shown in Fig. 11, gives the value of Q (principal stress) = σ_y at point B. This is true since $\sigma_y = 0$ at point '0'. Q = area under curve times scale factor = 11.65 x 2000 x 1/6 = 3880 p.s.i.

For finding the principal stress at point 'B' by graphical integration, the Lamé transformation equation, $P = P_o - \int(P-Q)\cot\psi \, d\theta$,* was used. The integration was performed along the stress trajectories A'B and AB.** P_o, the stress at A' (or A) is given by the fringe order at that point since it lies on the boundary at a point that is not externally loaded. The stations were chosen for constant increment of $\delta\theta$ = 10 degrees 0.1745 radians. For each station, (P-Q) was given by the fringe order and ψ was measured by rotating the stress trajectory counterclockwise to bring it on the isoclinic at that point. The necessary data for ϕ = 90 degrees and a/d = 1.25 are presented in tabular form in tables 4 and 5, and the required integrals are shown graphically in Figures 12 and 13.

For integration along stress trajectories AB and A'B, Q was found to be 3520 p.s.i. and 3240 p.s.i. respectively.

Integration along three separate lines gave the values of principal stress at point B of 3240 p.s.i., 3520 p.s.i. and 3880 p.s.i. These results show a variation of about plus or minus 9% from the arithmetic mean.

---

*Lamé-Maxwell equation, see Photoelasticity, Vol. I, by M. M. Frocht, pp. 54-66 and p. 287, John Wiley & Sons, Inc., N. Y.

**Lines A'B and AB actually deviate slightly from the stress trajectory due to the friction between the surfaces of the pin and hole. The error is small enough to be neglected. See Frocht[10].

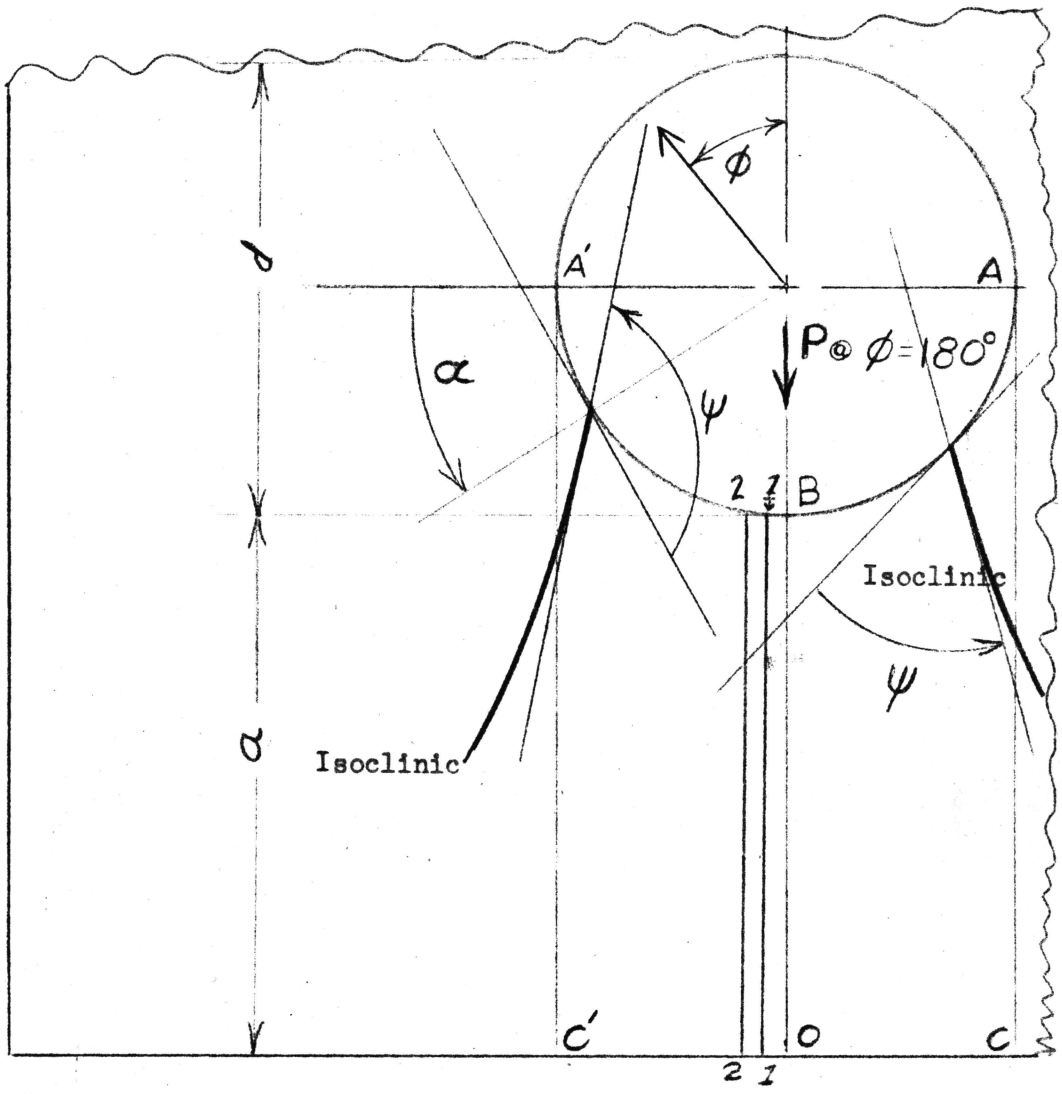

Fig. 7.

Sketch explaining notation used.

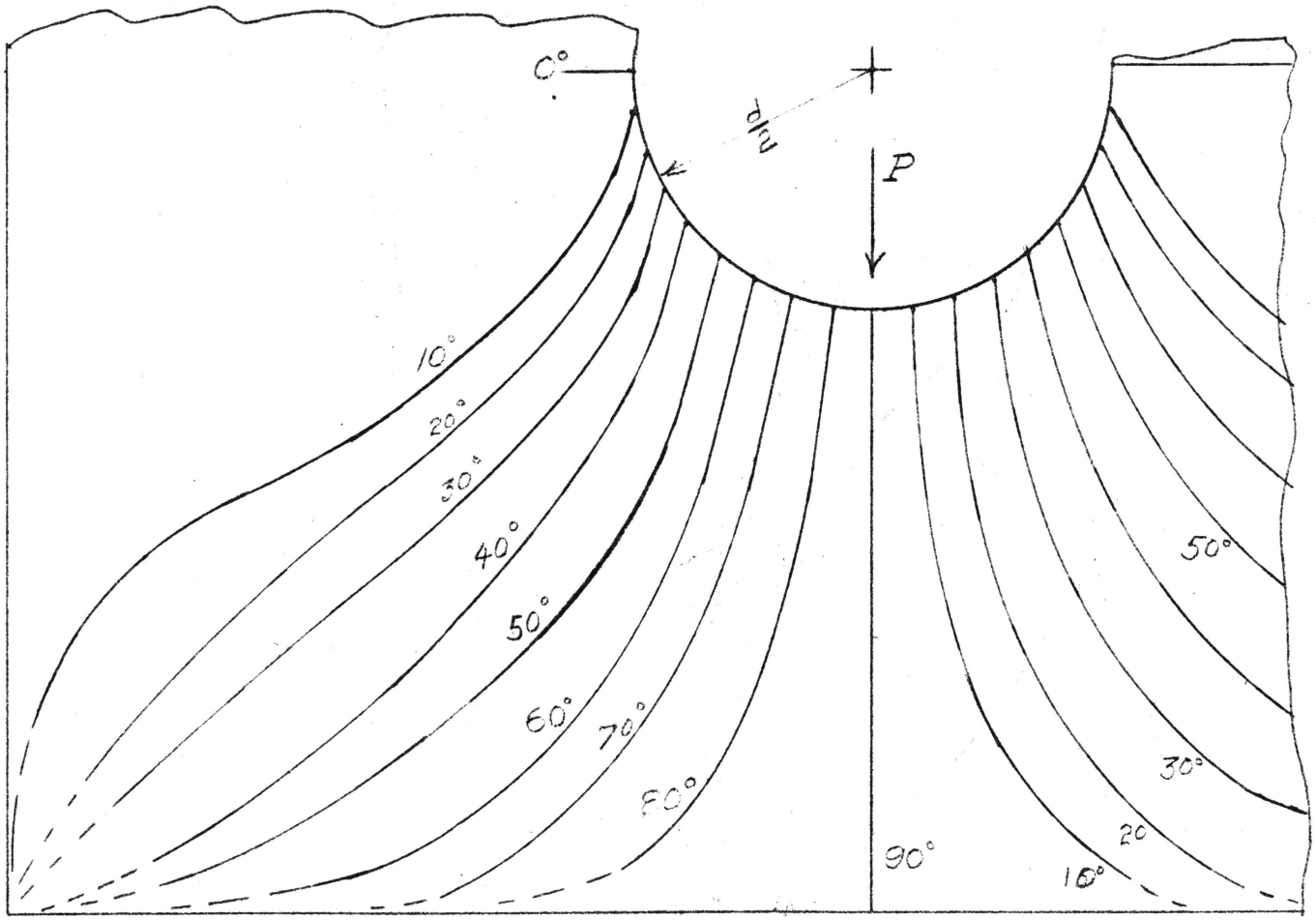

Fig. 8.
Isoclinics for ϕ =90° (180°)

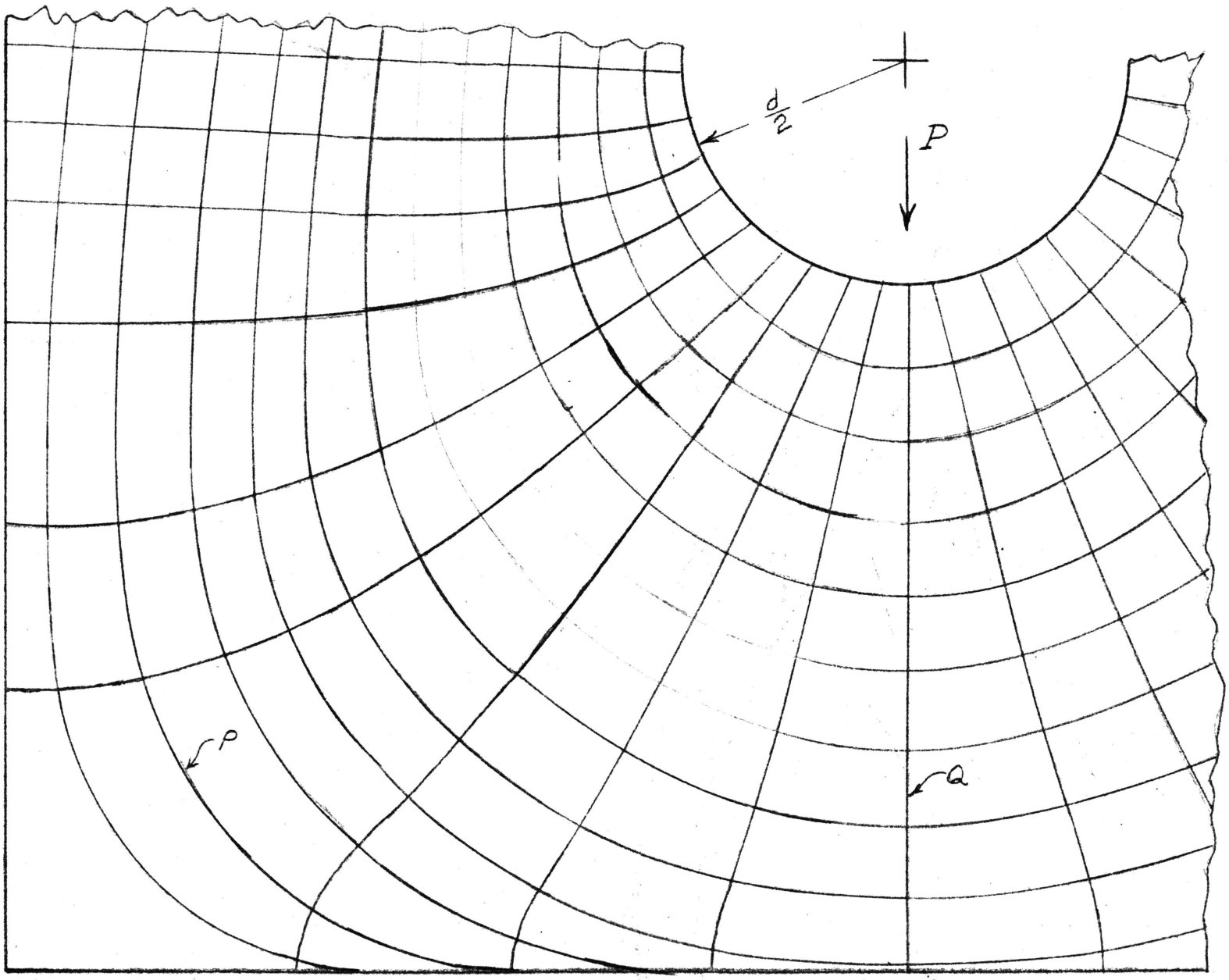

Fig. 9. Stress trajectories for $\phi = 90^\circ$ (180°)

Table 2.

Data for shear stress calculations on sections A'C' and AC. (See Fig. 10.)

Section A'C'							Section AC						
S_{t_a}	b fringe order	$\frac{P-Q}{2}$	θ_y	$2\theta_y$	Sine $2\theta_y$	τ_{xy}	S_{t_a}	b	$\frac{P-Q}{2}$	θ_y	$2\theta_y$	Sine $2\theta_y$	τ_{xy}
1C'	3.2	535	0°	-	-	0	1-C	2.8	467	-	-	-	0
2	3.2	550	15	30°	0.5	275	1	3.3	550	12	24	0.406	224
3	3.7	628	20	40	0.65	405	2	3.9	652	15	30	0.50	326
4	4.4	785	25	50	0.766	600	3	4.7	785	19	38	0.616	482
5	5.0	835	28	56	0.83	692	5	5.6	935	25	50	0. 644	600
6	5.9	985	30	60	0.866	855	6	6.9	1150	29	58	0.743	852
7	6.9	1160	37	72	0.95	1100	7	8.2	1330	30	60	o.866	1190
8	8.1	1350	43	86	0.999	1348	8	9.9	1652	34	68	0.927	1530
9	9.3	1550	47	94	0.999	1500	9	11.8	1970	38	76	0.999	1910
10	10.5	1750	54	1008	0.95	1660	10	16	2670	51	102	0.98	2250
11	11	1830	60	120	0.866	1580	11	16	2670	60	120	o.866	2310
12	11	1830	65	130	0.766	1400	12	16.3	2720	65	130	0.766	2080
13	10	-	-	-	0	0	13	-	-	-	-	-	0

CURVES for VARIATION of VERTICAL SHEAR SRRESS

along SECTIONS A'C' and AC for ϕ=90(180) deg.

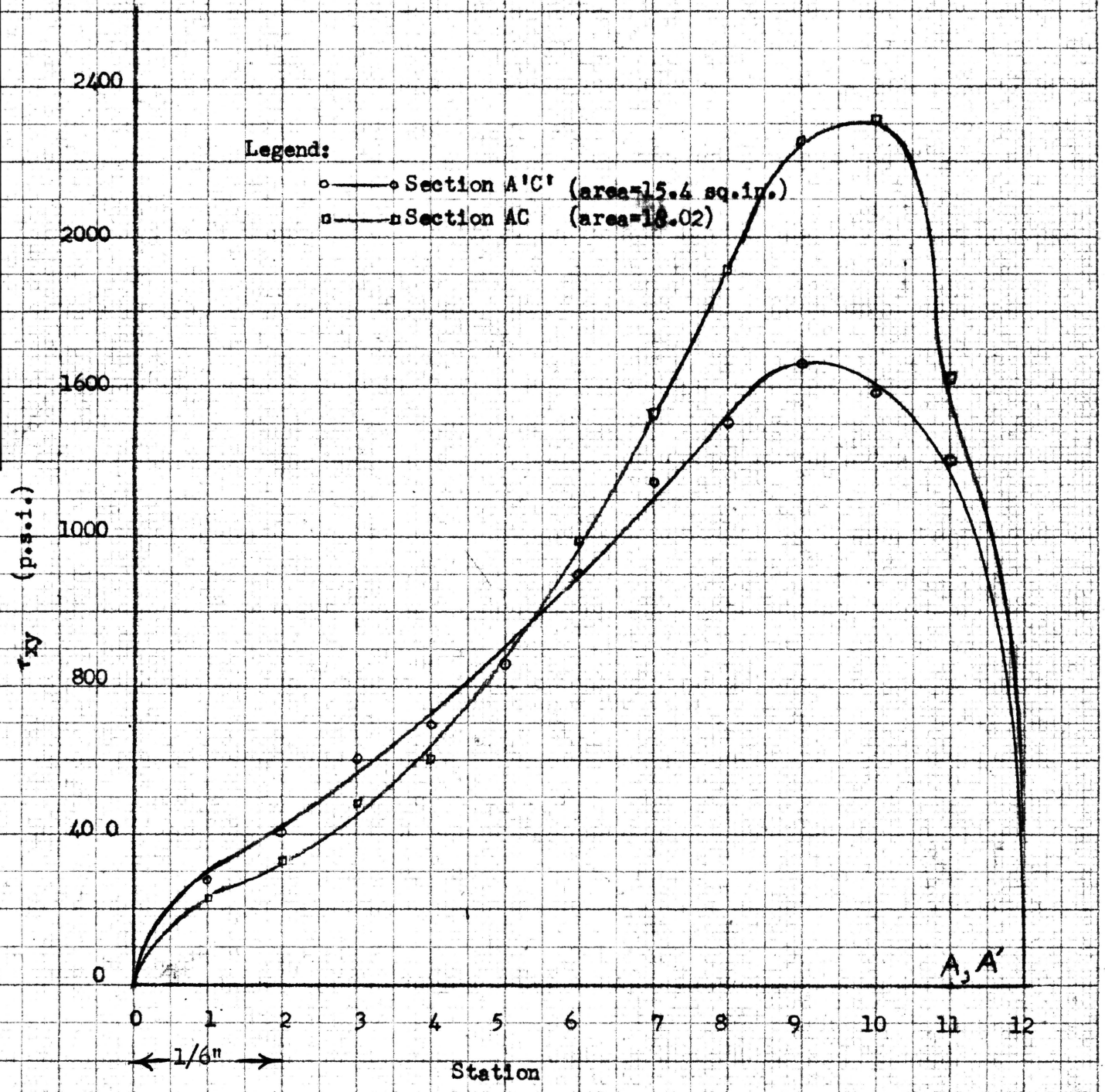

Fig. 10.

Table 3.

Data for rapid integration along trajectory OB.

	Section 1-1					Section 2-2							
$S_{t_{a.}}$	b	θ_y	Sine $2\theta_y$	bF	$(\tau_{xy})_1$	b	bF	θ_y	Sine $2\theta_y$	$(\tau_{xy})_2$	$2(\tau_{xy})_1$	$\frac{(\tau_{xy})_2}{2}$	$\frac{\partial(\tau_{xy})}{\partial_x}$
0	2.1	0	0	-	0	2.0	-	0	0	-	-	-	-
1	2.2	86	0.139	380	52.8	2.1	362	85	0.174	63	106	32.5	1720
2	2.4	85	0.174	415	71.6	2.3	397	83	0.250	98	143.2	49	2260
3	2.6	84	0.208	450	93.6	2.5	431	81	0.309	134	187.2	67	2880
4	2.8	83	0.242	484	117	2.7	465	79	0.374	174	234	87	3530
5	3.0	82	0.276	518	143	2.9	500	77	0. 438	220	286	110	4230
6	3.9	81	0.309	674	208	3.8	655	75	0.500	327	416	163.5	6060
7	4.7	79	0.374	810	303	4.6	793	72	0.580	460	606	230	9010
8	5.8	77	0.428	1000	428	5.6	965	68	0.695	670	856	335	12100
9	6.0	75	0.500	1070	535	6.0	1030	64	0.786	810	1070	405	15700

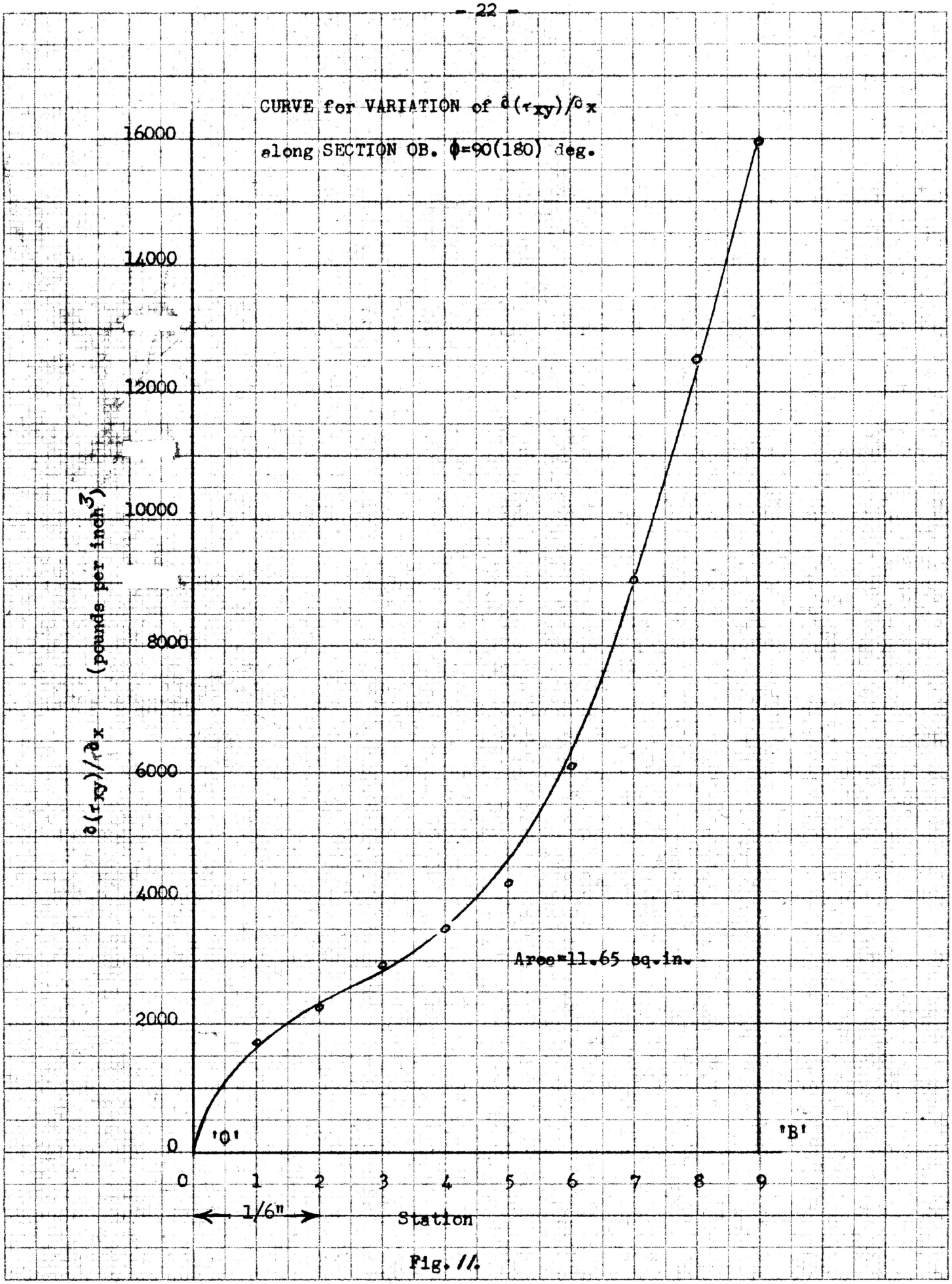
CURVE for VARIATION of $\partial(\tau_{xy})/\partial x$
along SECTION OB. ϕ=90(180) deg.
16000
14000
12000
10000
8000
6000
4000
2000
0
$\partial(\tau_{xy})/\partial x$ (pounds per inch^3)
'O'
'B'
0
1
2
3
4
5
6
7
8
9
1/6"
Station
Area=11.65 sq.in.

Fig. 11.

Tables 4 & 5.

Data for graphical integration along trajectories A'B and AB. (See fig. 12) Φ=90(18 0) degrees.

Section A'B					
α	b	P-Q	ψ	cot. ψ	(P-Q)cot. ψ
$^{0}A'$	6.5	2240	90	0	0
10	7.0	2420	150	1.73	4220
20	7.7	2660	152	1.88	5000
30	8.0	2760	140	1.19	3300
40	9.0	3100	120	0.84	2600
50	9.0	3100	115	0.465	1450
60	8 .0	2760	107	0.306	843
70	6.8	2320	99	0.158	368
80	6.0	2080	94	0.07	160
90 B	6.2	2140	90	0	0

Section AB					
α	b	P-Q	ψ	cot. ψ	(P-Q)cot. ψ
180 A	7.0	2420	90	0	0
170	8.0	2760	34	1.48	4750
160	8.5	2930	35	1.42	5500
150	9.0	3100	46	0.98	3660
140	10.	3450	58	0.63	3250
130	9.0	3100	65	0.42	1430
120	8.0	2760	73	0.306	850
110	7.5	2580	81	0.158	250
100	7.0	2420	86	0.070	160
90 B	6.2	2140	90	0	0

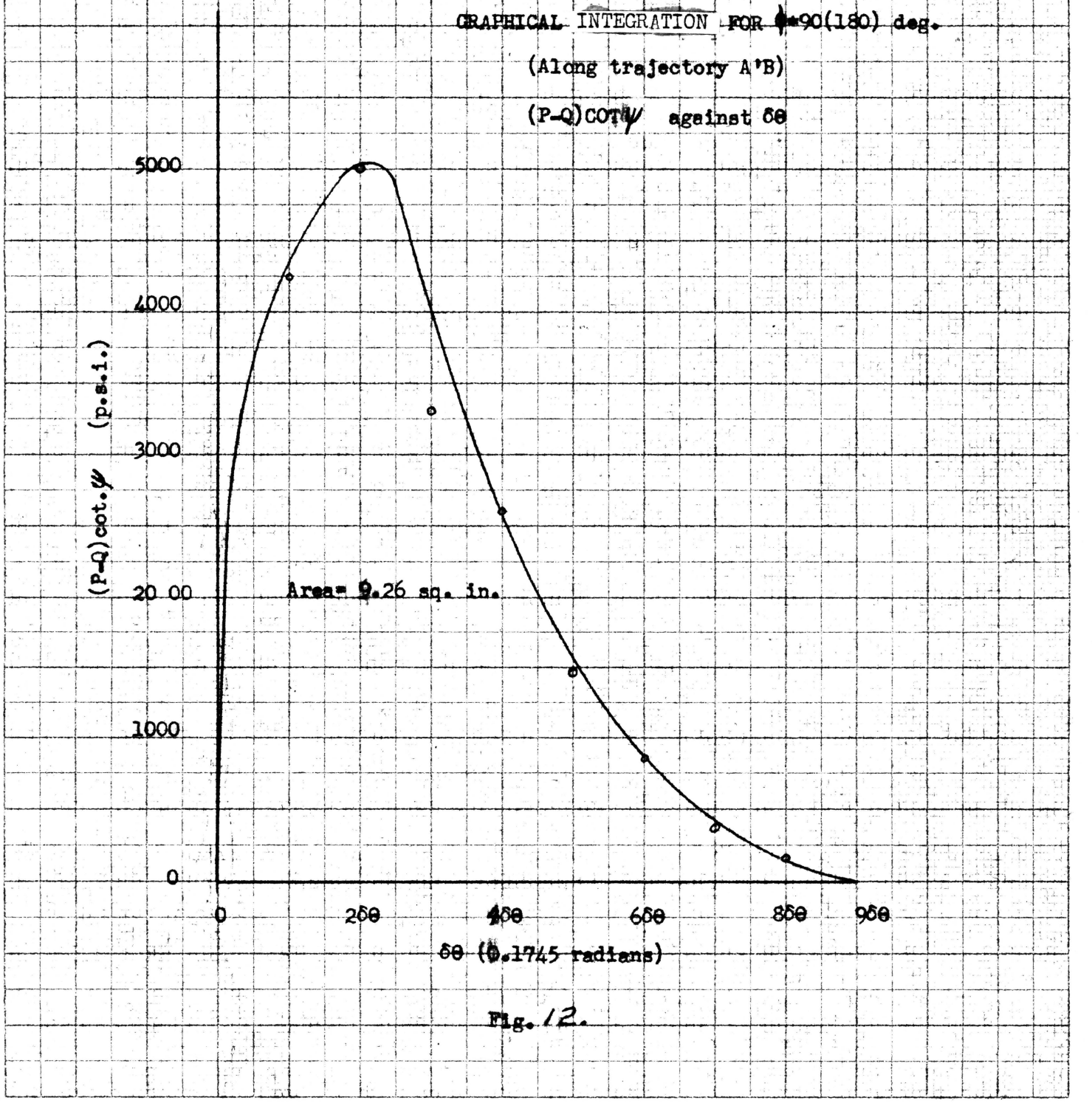
GRAPHICAL INTEGRATION FOR ψ=90(180) deg.
(Along trajectory A'B)
(P-Q)COTψ against δθ
5000
4000
3000
20 00
1000
0
(P-Q)cot.ψ (p.s.i.)
Area= 9.26 sq. in.
0
2δθ
4δθ
6δθ
8δθ
9δθ
δθ (0.1745 radians)

Fig. 12.

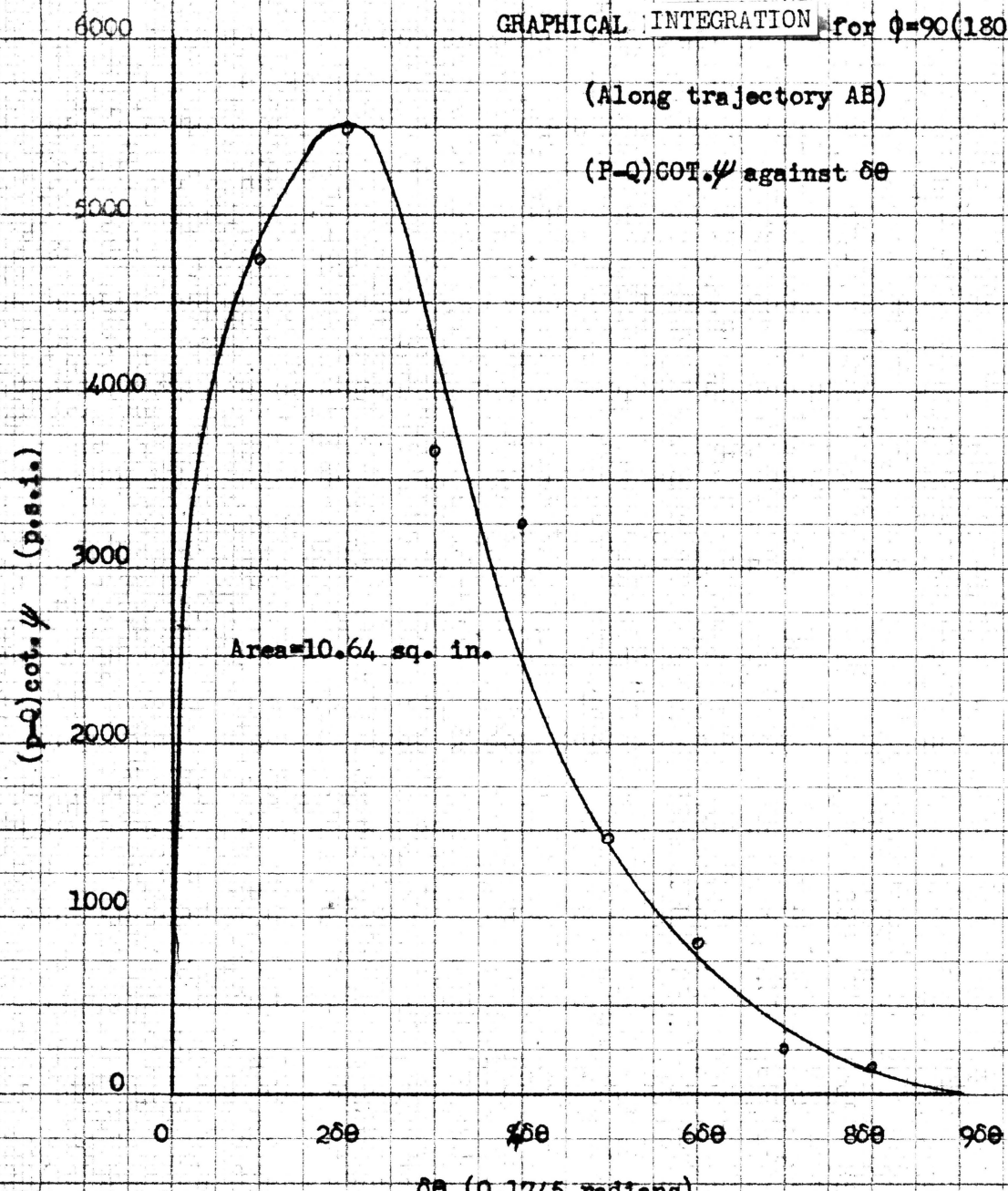
GRAPHICAL INTEGRATION for ϕ=90(180) deg.
(Along trajectory AB)
(P-Q)COT.ψ against δθ
6000
5000
4000
3000
2000
1000
0
(P-Q)cot. ψ (p.s.i.)
Area=10.64 sq. in.
0
2δθ
4δθ
6δθ
8δθ
9δθ
δθ (0.1745 radians)

Fig. 13.

Table 7.

Data for graphical integration along trajectory GH(see fig.14). ϕ= 135 deg.

α deg.	ψ deg	cotψ	b	P-Q	(P-Q)cot
0(G)	90	0	4	1450	0
10	152	1.88	4.4	1610	3020
20	146	1.48	4.7	1720	2540
30	133	0.78	5.0	1830	1440
40	122	0.63	5.3	1940	1240
50	113	0.41	5.7	2080	855
60	106	0.29	6.2	2260	655
70	97	0.123	6.8	2480	350
80	92	0.044	6.9	2500	110
90	90	0	7.0	2560	0

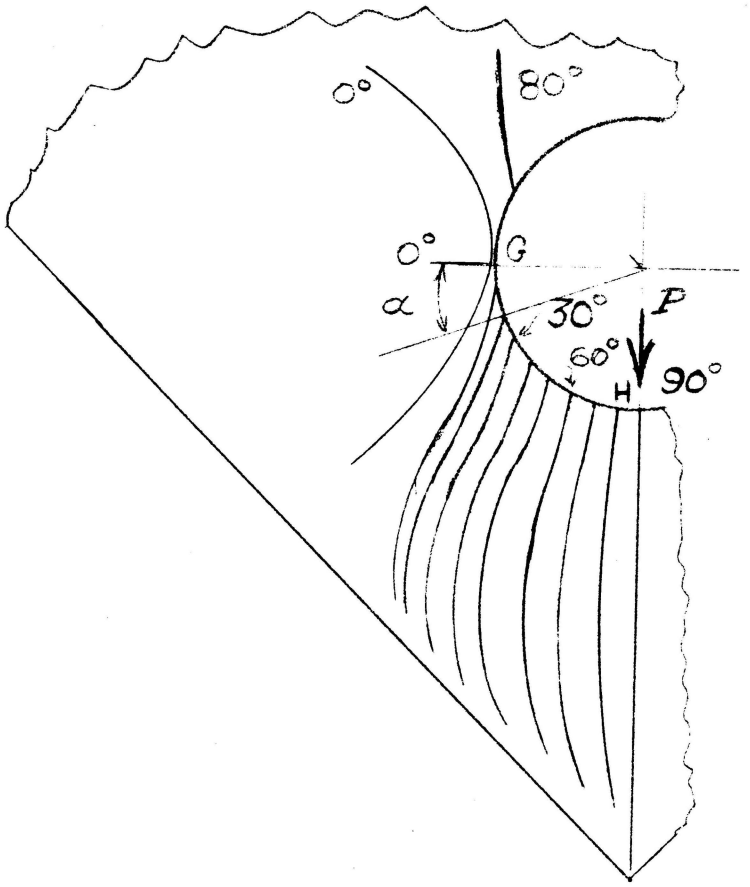

Fig. 14.
Sketch of isoclinics for ϕ= 135 degrees.

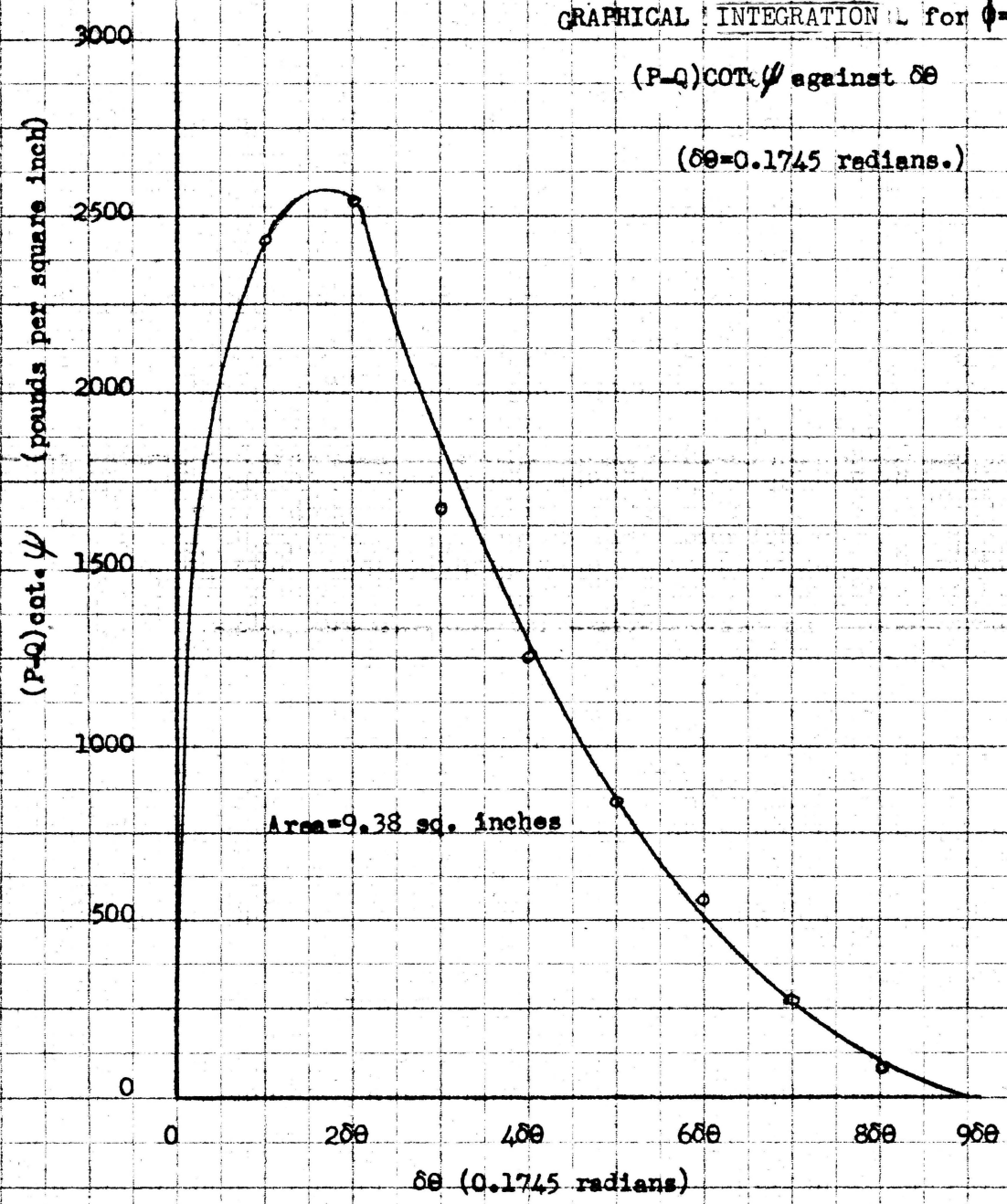
GRAPHICAL INTEGRATION for ϕ=45(225) deg.
(P-Q)COTψ against $\delta\theta$
($\delta\theta$=0.1745 radians.)
(P-Q)cot.ψ (pounds per square inch)
3000
2500
2000
1500
1000
500
0
Area=9.38 sq. inches
0
2$\delta\theta$
4$\delta\theta$
6$\delta\theta$
8$\delta\theta$
9$\delta\theta$
$\delta\theta$ (0.1745 radians)

Fig. 15.

Table 6.

Data for graphical integration along trajectory EF (See fig.16). ϕ= 45 deg.

α deg.	ψ	cot. ψ	b	P-Q	(P-Q) cot.
0(E)	90.0	0	3	1090	0
10	154	2.03	3.2	1200	2430
20	148	1.88	3.7	1350	2540
30	138	1.10	4.1	1500	1680
40	128	0.78	4.4	1000	1250
50	119	0.48	4.7	1720	835
60	108	o.309	5.0	1830	565
70	98	0.139	5.3	1940	270
80	92	0.139	5.6	2040	81
90	90	0	6.0	2190	0

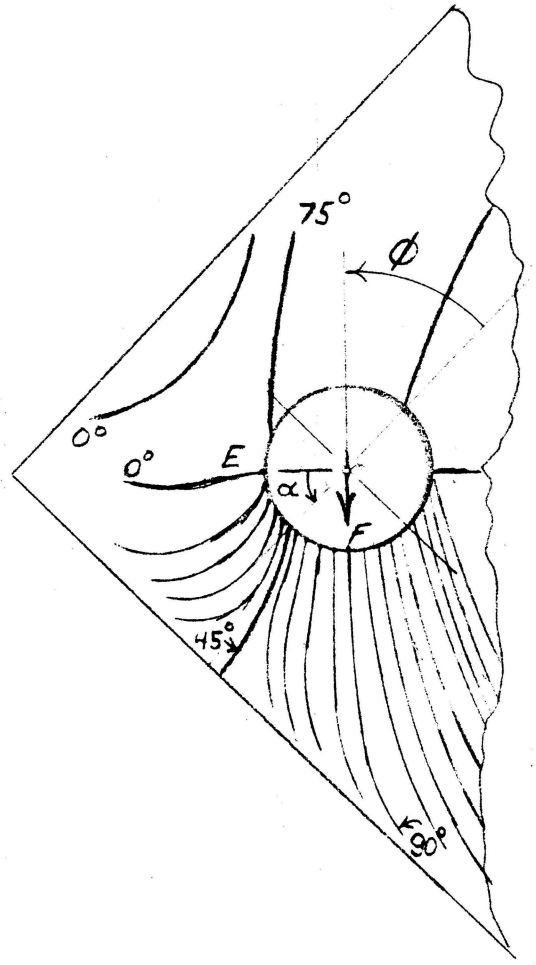

Fig. 16.

Isoclinics for ϕ=45 (225) degrees.

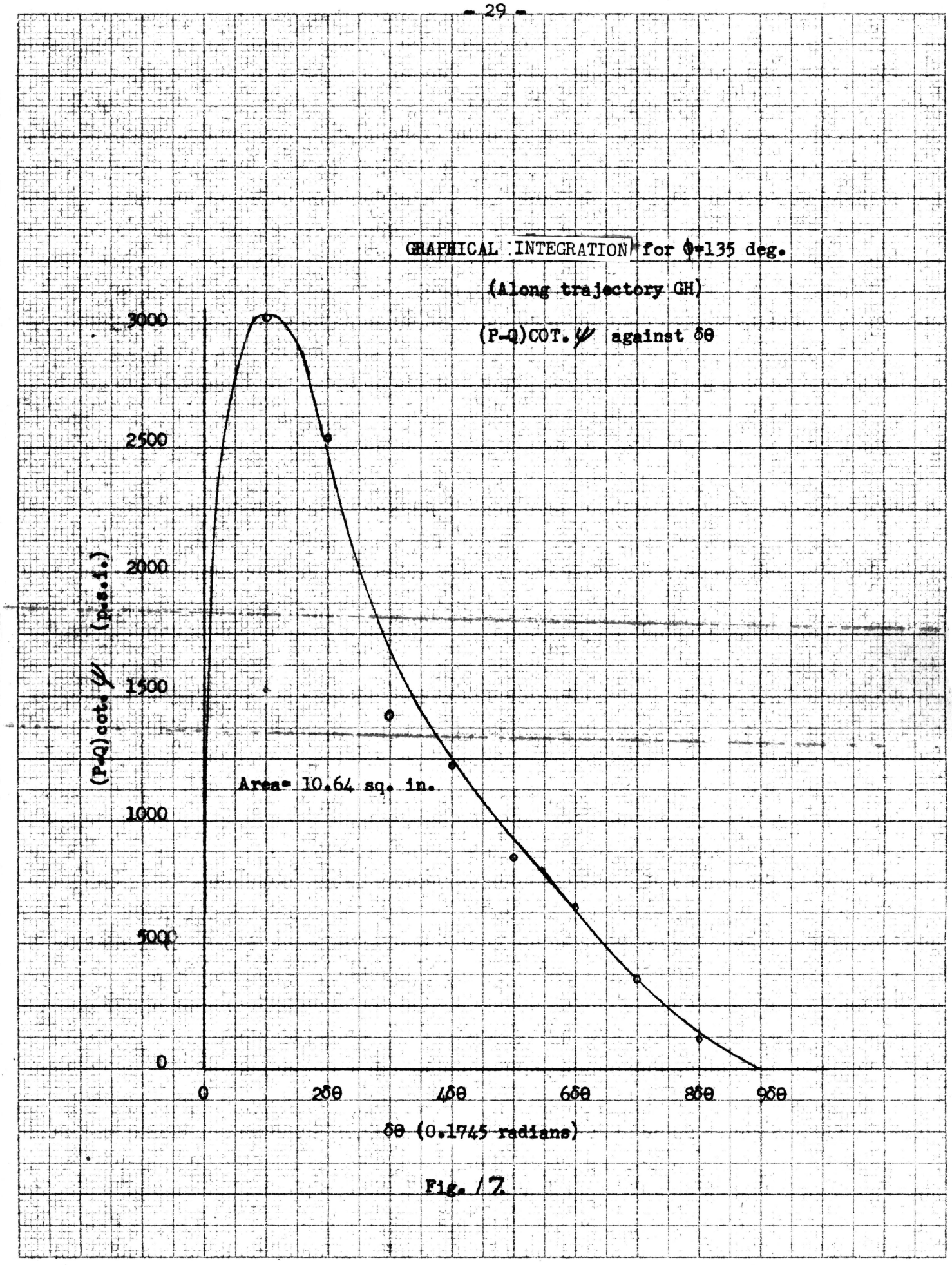
GRAPHICAL INTEGRATION for ϕ=135 deg.
(Along trajectory GH)
(P-Q)COT. ψ against δθ
3000
2500
2000
1500
1000
500
0
(P-Q) cot. ψ (p.s.i.)
Area= 10.64 sq. in.
0
2δθ
4δθ
6δθ
8δθ
9δθ
δθ (0.1745 radians)

Fig. 17

V. DISCUSSION OF RESULTS

Results presented in Figures 1, 2 and 3 show that the values of tensile, compressive and shear stresses vary inversely with a/d. To use the curves in predicting the stresses which will occur, it is necessary to know the shear stress, P/A, on the rivet or bolt. For example, assume P/A is 10,000 p.s.i., and it is desired to know what the maximum marginal tensile stress will be for a load angle of ϕ = 90 degrees with a/d = 1.40. In Fig. 2, use appropriate curve and find the S.C.F.(T) to be 2.25. By multiplying 2.25 x 10,000, the maximum tensile stress is found to be 22,500 p.s.i. This procedure may be followed for all S.C.F. versus a/d curves.

VI. CONCLUSIONS

Results of this investigation show that the recommendations for a minimum a/d ratio of 1.5 is justified in the design of margin widths.

For an a/d = 1.5 in a riveted joint in which the average rivet shear stress, (P/A) is 15,000 p.s.i., the maximum shear stress in the plate for ϕ = 45 (225) degrees is 1.35 x 15,000 = 20,220 p.s.i. The shearing yield strength for structural steel is about 21,000 p.s.i.[12], which shows the margin of safety to be very small. For the same load condition, the maximum tensile stress in the plate is 1.6 x 15,000 = 24,000 p.s.i. and the maximum compressive stress is 2.1 x 15,000 = 31,500. Based on a yield point of 35,000 p.s.i.[12] the margin of safety for both tension and compression is higher than for shear, which shows that the shear is critical.

By steps similar to those used above, it can be shown that the compressive stress is critical for ϕ = 90 (180) degrees and ϕ = 135 degrees.

The optimum value for a/d depends on the properties of the material from which the plate is made and the direction of the applied load.

VII. ACKNOWLEDGEMENTS

The writer of this thesis wishes to express gratitude to Professor D. H. Pletta for his guidance throughout this investigation.

VIII. BIBLIOGRAPHY

1. Frocht, M. M. Photoelasticity. Vol. II. Chap. 6. John Wiley & Sons, Inc., New York.

2. Bickley, W. G. "Distribution of Stress Round a Circular Hole in a Plate". Phil. Trans. Royal Society, London. Vol. 227, A, pp. 383 - 415. 1928.

3. Knight, R. C. "Action of a Rivet in a Plate of Finite Breadth". Phil. Mag. Vol. 19 (7), pp. 517 - 540. March, 1935.

4. Coker, E. G. and Filon, L. N. G. A Treatise on Photoelasticity. Cambridge University Press. 1931. P. 525.

5. Seely, F. B. Resistance of Materials. Third Edition. P. 49. John Wiley & Sons, Inc., New York.

6. Bruhn, E. F. Analysis and Design of Airplane Structures. Chap. 4.6. Tri-State Offset Co. Cincinnati 2, Ohio.

7. Younger, J. E. Mechanics of Aircraft Structures, p. 378. McGraw-Hill Book Company, Inc., New York and London. 1942.

8. Marks, L. S. Mechanical Engineer's Handbook, p. 915. McGraw-Hill Book Company, Inc., New York and London.

9. Frocht, M. M. Photoelasticity. Vol. II, Section 6.7. John Wiley & Sons, Inc., New York.

10. Frocht, M. M. Photoelasticity. Vol. I, Ex. 9.4. John Wiley & Sons, Inc., New York.

11. Frocht, M. M. Photoelasticity. Vol. I, Section 6.1. John Wiley & Sons, Inc., New York.

12. Seely, F. B. Resistance of Materials. Table I. John Wiley & Sons, Inc., New York.